Direct Imaging and Chemical Identification of the Encapsulated Metal Atoms in Bimetallic Endofullerene Peapods

Rebecca J. Nicholls,[†,*] Kasim Sader,[‡] Jamie H. Warner,[†] Simon R. Plant,[†] Kyriakos Porfyrakis,[†] Peter D. Nellist,[†] G. Andrew D. Briggs,[†] and David J. H. Cockayne[†]

[†]Department of Materials, University of Oxford, Parks Road, Oxford, OX1 3PH U.K. and [‡]SuperSTEM Laboratory, STFC Daresbury, Keckwick Lane, Warrington WA4 4AD U. K.

ABSTRACT In this paper, a chemically sensitive local characterization technique is used to characterize fullerene peapods containing two metal atoms within each fullerene. By combining bright-field imaging, high-angle annular dark-field imaging, and electron energy loss spectroscopy in a scanning transmission electron microscope, unambiguous identification of the metal atoms present is possible. Key to making this possible is aberration correction, which allows atomic resolution at lower beam energies. The peapods can be imaged for several consecutive scans at 80 keV beam energy, and the combination of techniques allows the position as well as the species of the encapsulated atoms to be identified. Movements of the encapsulated atoms are monitored.

KEYWORDS: peapods · EELS · STEM

The ability to isolate single atoms and groups of atoms within fullerenes inside a nanotube has resulted in these endohedral fullerene peapod materials becoming one of the candidate materials for quantum information processing.[1] Endohedral fullerenes also have potential applications in magnetic resonance imaging[2] and organic photovoltaic devices.[3] The characterization of such endohedral fullerene peapod materials is extremely challenging because it requires techniques providing atomic resolution with chemical sensitivity. There have been attempts to synthesis bimetallic endohedral fullerene peapods which contain two different metals within the fullerene,[4] but to date, this material has only been studied using techniques that do not provide local information,[4] such as mass spectrometry, optical absorption, energy-dispersive X-ray spectroscopy, nuclear magnetic resonance spectroscopy, and electron paramagnetic resonance spectroscopy, and therefore do not allow the unambiguous identification of the encapsulated atomic species.

Techniques that can provide atomic resolution information are therefore crucial characterization tools for these materials. High-resolution transmission electron microscopy (HRTEM) is such a technique and has often been used for the characterization of peapods.[5,6] HRTEM is, however, essentially a phase contrast technique with a relatively weak compositional dependence. The technique of high-angle annular dark-field (HAADF) imaging in a scanning transmission electron microscope (STEM) shows a much stronger composition dependence and has long been shown to give clear contrast of single atoms on lighter supports.[7,8] The explanation is that the scattering to the relatively high angles involved in HAADF STEM is largely Rutherford scattering from the nuclear potential so has an intensity that varies strongly with atomic number (close to Z^2). A further advantage of using STEM is that the small illuminating spot or probe allows local spectroscopy, leading to chemical information. The energy lost by the incident electrons as they are transmitted through the sample shows features at characteristic energies arising from the excitation of core−shell electrons in the target atoms, allowing chemical identification.[9] Such electron energy loss spectra also show fine structure that can indicate the chemical environment of the species. A STEM instrument can also form phase contrast images similar to those seen in HRTEM, which allows the lower Z nanotube and fullerene cage to be imaged, although the efficiency of imaging in this mode is lower than that for HRTEM, leading to noisier images.

In this paper, we combine HAADF STEM imaging with electron energy loss spectroscopy (EELS) and phase contrast imaging to identify the species and location of the

*Address correspondence to rebecca.nicholls@materials.ox.ac.uk.

Received for review April 20, 2010 and accepted June 10, 2010.

Published online June 17, 2010. 10.1021/nn100823e

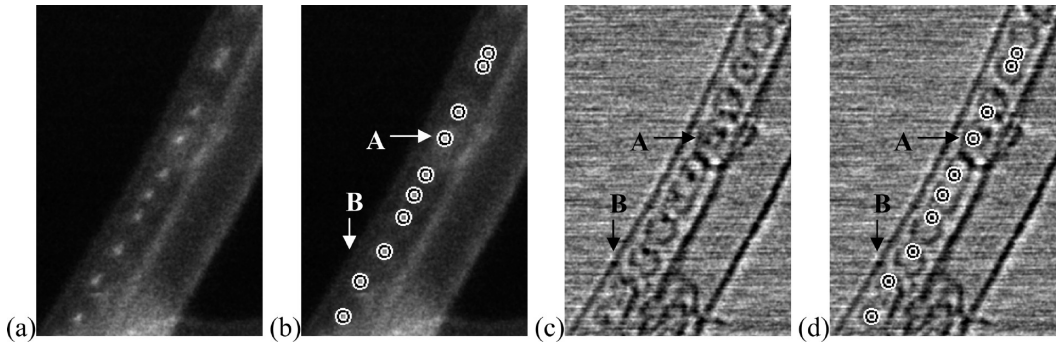

Figure 1. Simultaneously obtained dark-field (a,b) and bright-field (c,d) images with the La atom positions marked in (b) and (d). Dark spots in the bright-field image do not always coincide with the heavy atom positions from the dark-field image.

heavy encapsulated atoms in an endofullerene peapod structure. One of the difficulties of studying carbonaceous materials using TEM/STEM is that the samples suffer from beam damage, through either knock-on or ionization mechanisms. The rate of damage is sample-dependent and varies with the geometry of the sample.[10] Furthermore, both HAADF and phase contrast STEM are less efficient in their use of the incident electrons than HRTEM, and so for a similar signal-to-noise ratio, a higher electron fluence is required. There is some evidence, however, that the very small illuminating region in STEM allows greater dissipation of the deposited energy, leading to reduced damage.[11] For nanotube samples, the dominant damage mechanism is thought to be knock-on damage, which has a threshold energy just above 80 keV.[12] In cases where ionization damage dominates (*e.g.*, possibly crystals of fullerenes with a large band gap[13]), lower beam energies may increase the ionization damage. The situation for the damage in peapods is complicated. The possibility of coupling between ionizations on the fullerenes and the delocalized electrons on the nanotube may mean ionization damage to the fullerenes is not as severe as in the case of the fullerene crystal. With the possibility of knock-on and ionization damage, a compromise voltage is preferable. Several groups have recently used beam energies of 80 keV or lower to study these and similar materials to try to reduce the knock-on damage.[14−17] Although these are relatively low compared to the beam energies typically used for atomic resolution imaging, the recent development of correctors for the inherent spherical aberration of electron lenses[18] allows single atoms to still be observed in a STEM at a beam energy of 80 keV. The work presented here has been carried out on an aberration-corrected VG STEM operated with a beam energy of 80 keV. It was found that the peapod structures remained visibly intact long enough to monitor the motion of the encapsulated atoms with time, and in general, at least eight consecutive scans could be obtained without being able to observe any damage. Spectrum line scans, however, were found to have no visible effect on the nanotubes but caused the fullerenes to fuse together.

Using the techniques described above, the position and species of the encapsulated atoms are determined, and this information allows a reinterpretation of the structure of the endohedral fullerene.[4] Furthermore, the dynamics of the atoms are monitored under the beam irradiation.

RESULTS AND DISCUSSION

Figure 1 shows HAADF STEM and simultaneously recorded bright-field (phase contrast) images from a sample of La@C_{82} fullerene peapods. By the principle of reciprocity,[19] the phase contrast images recorded in STEM are equivalent to those that would be formed in the HRTEM. The HAADF image unambiguously shows the location of the metal atoms. By comparing the images, it can be seen that in many cases the metal atoms are also clear in the phase contrast image. In a number of places, however, the metal atoms are not immediately identifiable, and contrast arising from the carbon cage may be erroneously interpreted as metal atoms.

HAADF and bright-field images obtained simultaneously from supposed PrSc@C_{80} fullerenes[4] encapsulated inside a multi-walled nanotube are shown in Figure 2a,b, respectively, together with a second bright-field image in Figure 2c. The second bright-field image was recorded at a slightly different focus to the HAADF image because the bright-field image recorded under the same conditions as an optimally focused dark-field image has very little contrast. By defocusing the image, the contrast increases and the carbon structure becomes clearer. The combination of bright-field and HAADF images reveals two heavy atoms inside a single fullerene.

The question then arises as to whether Pr and Sc species can be separately identified. Pr and Sc have atomic numbers of $Z = 59$ and 21, respectively, and consequently, since in HAADF imaging the image in-

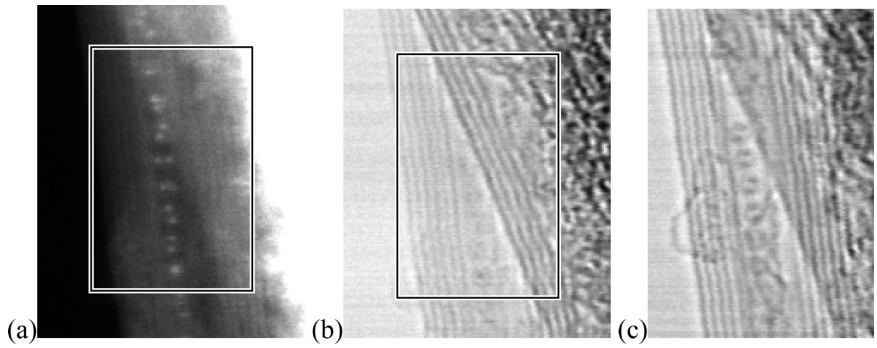

Figure 2. Corresponding HAADF (a) and bright-field (b) images of $PrSc@C_{80}$ molecules encapsulated inside a multi-walled carbon nanotube along with a defocused bright-field image (c).

tensity is approximately proportional to Z^2, it should be possible to differentiate between the two atoms. Figure 3 shows a typical intensity profile across two encapsulated atoms. Since the intensity difference between two atoms within the same fullerene was found to be less than 10% (which is not significantly above the noise level), we conclude that the atoms have very similar atomic numbers, even taking into account the possible movement of the encapsulated atom out of the electron probe as reported by Suenaga *et al.*[16] It is also possible to see spots of higher intensity in Figure 3. These are caused by the fullerenes rotating into positions where the two heavy metal atoms are on top of each other when viewed in projection.

To determine the atomic species, EELS spectra were obtained from the peapods, an example spectrum being shown in Figure 4. The Pr N-edge at 113 eV is visible in the spectrum, and a profile of how the background subtracted intensity of the Pr edge changes with position is shown in Figure 4c. No Sc $L_{2,3}$-edge at 402 eV is observed. Scanning the beam over a small area of the peapod repeatedly and obtaining a cumulative spectrum (Figure 4d) still showed no Sc signal.

From the HAADF images and the EELS spectrum, we can conclude that both atoms are Pr. This suggests a reinterpretation of the original identification of this material as $PrSc@C_{80}$,[4] which was based upon mass spectrometry and EDX measurements, and highlights the importance of combining local chemically sensitive characterization methods with other characterization techniques. Re-examination of the EDX data from ref 4 shows it to be consistent with the HAADF and EELS reported here (see Supporting Information). Also, the mass spectrometry results in ref 4 can be interpreted in terms of $Pr_2@C_{72}$ (with a mass of 1146) rather than $ScPr@C_{80}$ (which has also a mass of 1146). Two Pr atoms would be consistent with the isotopic distribution shown in ref 4 as Pr, like Sc, is monoisotropic. C_{72} is an unusual but not an unknown cage, and $La_2@C_{72}$[20−22] and $Ce_2@C_{72}$[23] have both been reported. The UV−vis−IR spectrum in ref 4 is similar in shape to that reported for $La_2@C_{72}$ and $Ce_2@C_{72}$.[22] The ^{13}C NMR spectra for $La_2@C_{72}$[20] and $Ce_2@C_{72}$[23] are different from each other, as well as to that obtained in ref 4. It should be noted that the imaging and spectroscopy presented in this paper and the EDX and mass spectrum results presented in ref 4 would be consistent with a fullerene $Pr_2C_2@C_{70}$ as well as $Pr_2@C_{72}$. More work is needed, however, to elucidate unambiguously the fullerene cage structure.

In previous work by Ding and Yang,[24] Pr has been found to exist in a valence state of +3 in both $Pr@C_{82}$ and $Pr_2@C_{80}$. The Pr spectrum shown in Figure 4c shows a double peak structure. $N_{4,5}$-edges of rare earth metals have been used in the past to learn something about the valence state of the rare earth ion.[25] The double peak structure is closer to the spectrum obtained by Trebbia and Colliex from Pr metal[26] than that obtained by Ahn and Krivanek[27] for Pr_6O_{11}. As the process of obtaining spectra from the fullerenes changes them, it is

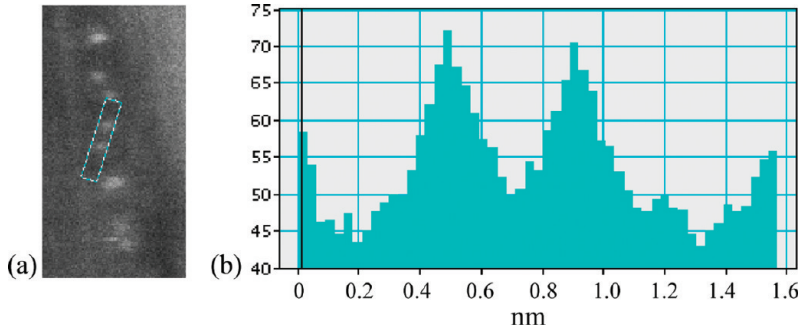

Figure 3. Intensity profile (b) across two encapsulated atoms in a HAADF image (a).

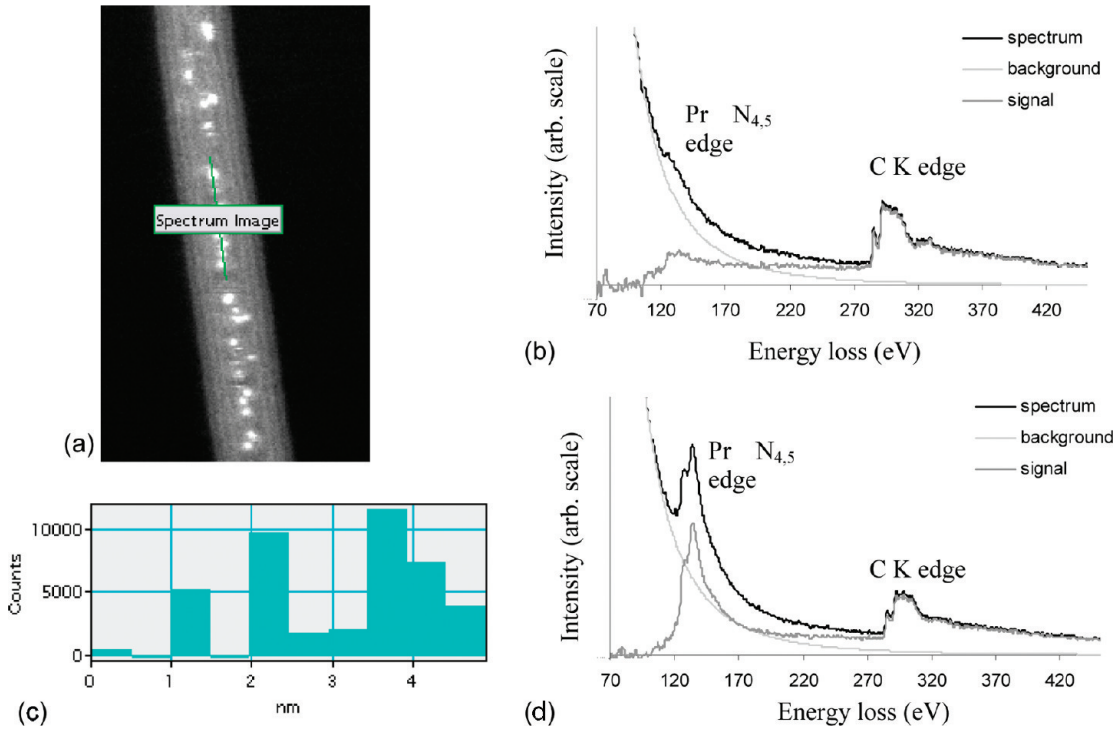

Figure 4. HAADF image showing the line used for spectrum image (a) and a typical spectrum (b). (c) Profile showing how the intensity of the background-subtracted Pr edge varies with position along the spectrum image. (d) Cumulative spectrum.

not possible to correlate this spectrum with a specific structure. It is likely that the Pr atoms in this case have the same valence state inside the fullerene as in the fullerenes studied by Ding and Yang, but that as the fullerene cages are destroyed in the process of taking the spectra, the Pr atoms escape from the fullerenes and are metallic in character.

The distance in the image between the two encapsulated atoms is a projection of the actual distance. The largest distance found was 0.55 ± 0.02 nm, indicating that the atoms are at least 0.55 ± 0.02 nm apart. From Figure 2, it can be seen that there are fullerenes with the Pr−Pr axis approximately perpendicular and parallel to the tube axis. Under the beam, the Pr−Pr axis orientation changes with time (including orientations where the images of the two atoms overlap), as can be seen in Figure 5. The last image in the series, at 374 s, shows damaged fullerenes. Rather than just relying on the dark-field image to check the damage, the simultaneously obtained bright-field image is also used to monitor the damage. The bright-field image in Figure 2c was obtained after the first three images shown in Figure 5, confirming that the fullerenes are still intact.

To investigate the orientation further, we have looked at the angle between the Pr−Pr axis and the tube axis, in a similar manner to the work by Suenaga *et al.*[5] and Khlobystov *et al.*[28] Values of φ (modulo 90°) have been recorded for the multi-walled tube shown in Figure 2 and for a double-walled tube where the fullerenes were more constrained. The results are shown in Figure 6, and although the number of tubes it was possible to analyze was rather small, the data do suggest that there may be some preferred orientations. There are two sources of error in these data. The first comes from the small number of cases recorded, and

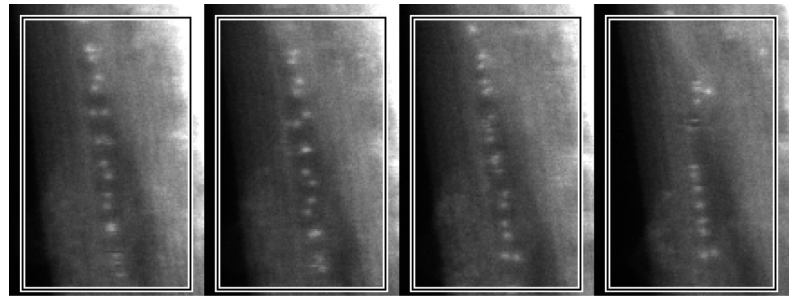

Figure 5. Series of images showing changes with time under the beam taken at 0, 87, 154, and 374 s (the fullerenes are damaged in the last image).

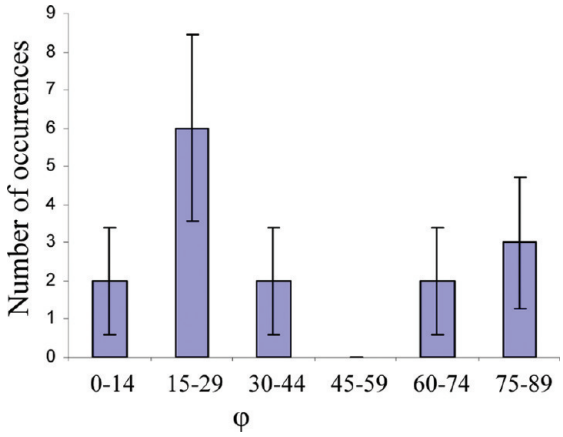

Figure 6. Histogram of the distribution of φ, the angle between the Pr−Pr axis, and the tube wall.

this error is quantified by Poisson statistics and marked onto the histogram in Figure 6. The second possible source of error is that all but three of the 15 measured φ values come from a multi-walled tube, which may not be representative of a tightly packed double-walled tube.

Values of φ were recorded for a single fullerene inside a double-walled nanotube over approximately 5 min in order to monitor the dynamics of the encapsulated atoms. The bright-field images were used to monitor the damage to the fullerenes and to confirm that they had not coalesced. The values of φ ranged from 0 to 21°, and no correlation was found between φ and the Pr−Pr distance. Images of this fullerene taken at larger time intervals show φ values of 68 and 75°, showing that over time the value of φ is not restricted to 0−21°.

The impossibility of distinguishing between the two atoms means that the two atoms could exchange places between two consecutive images, while the φ value appears not to change very much. Although we can see that the encapsulated atoms are moving, it is not possible to tell whether the encapsulated fullerene is rotating or whether the atoms are moving within the fullerene.

As well as neatly filled nanotubes, it was also possible to find nanotubes filled with wires containing heavy atoms and more unusual structures (Figure 7). The structure encapsulated inside the nanotube in Figure 7 is ill-defined and could be the result of beam damage. The combination HAADF and EELS allows us to identify groups of Pr atoms within the structure.

CONCLUSION

In this paper, a chemically sensitive local characterization technique, combining HAADF imaging, bright-field imaging, and EELS spectroscopy, has been used to identify the metals present in a bimetallic endofullerene peapod material originally thought to contain PrSc@C_{80} fullerenes. Aberration correction has allowed the characterization to be carried out at a low voltage, which reduces the beam damage while maintaining resolution. The EELS signal from Pr has been detected, and the movements of the encapsulated atoms have been monitored using HAADF imaging. The absence of a Sc EELS signal and equal intensity of the encapsulated atoms in the HAADF images suggest that the endofullerene

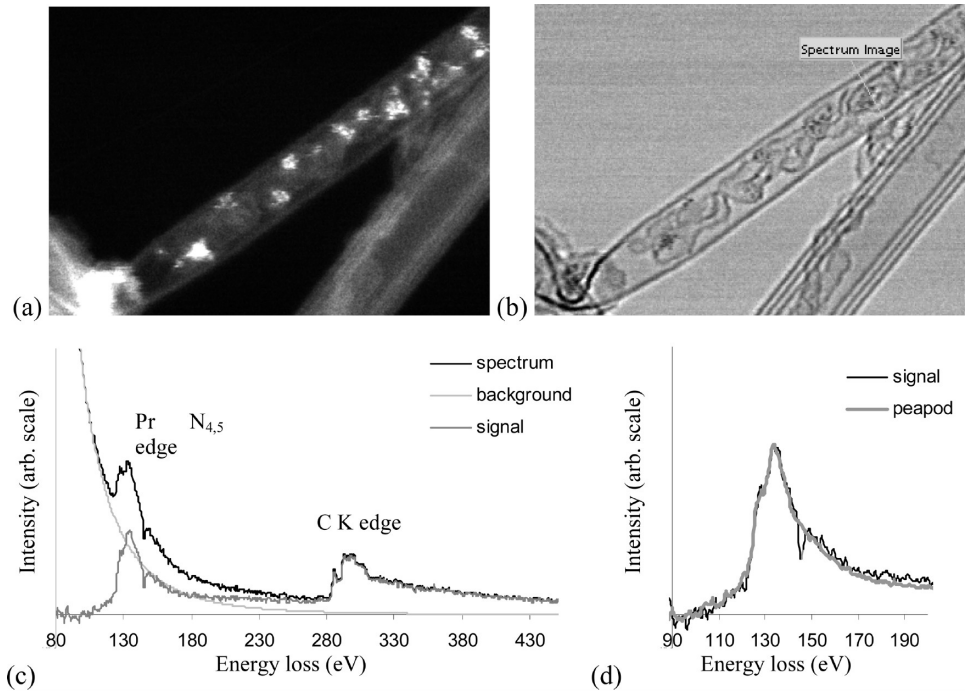

Figure 7. (a) HAADF image and (b) bright-field image showing line used for spectrum image. One of the spectra is shown in (c), and the Pr signal is compared to the cumulative peapod spectrum in (d).

contains two Pr atoms. With re-evaluation of the previous EDX and mass spectrometry results, this material is now interpreted as a fullerene containing two Pr atoms and 72 carbon atoms. This demonstrates the power and importance of using local characterization techniques to determine the species and position of heavy metal atoms in carbon nanomaterials.

METHODS

In this study, the peapod sample has been characterized using an aberration-corrected VG HB501 STEM (the Daresbury SuperSTEM1) operated with a beam energy of 80 keV, a convergence semiangle of 24 mrad, and a HAADF annular detector angle of 70−210 mrad. In general, at least eight consecutive scans (1024 × 1024 pixels and 19.5 μs dwell time) could be obtained without being able to observe any damage. Spectrum line scans, with 0.5 s acquisition time, were found to have no visible effect on the nanotube but caused the fullerenes to fuse together.

Acknowledgment. The authors would like to acknowledge the support of the Department of Materials, University of Oxford, and the UK Engineering and Physical Sciences Research Council.

Supporting Information Available: EDX spectra simulations. This material is available free of charge *via* the Internet at http://pubs.acs.org.

REFERENCES AND NOTES

1. Benjamin, S. C.; Ardavan, A.; Briggs, G. A. D.; Britz, D. A.; Gunlycke, D.; Jefferson, J.; Jones, M. A. G.; Leigh, D. F.; Lovett, B. W.; Khlobystov, A. N.; *et al.* Towards a Fullerene-Based Quantum Computer. *J. Phys.: Condens. Matter* **2006**, *18*, S867–S883.
2. Kato, H.; Kanazawa, Y.; Okumura, M.; Taninaka, A.; Yokawa, T.; Shinohara, S. Lanthanoid Endohedral Metallofullerenols for MRI Contrast Agents. *J. Am. Chem. Soc.* **2003**, *125*, 4391–4397.
3. Ross, R. B.; Cardona, C. M.; Guldi, D. M.; Sankaranarayanan, S. G.; Reese, M. O.; Kopidakis, N.; Peet, J.; Walker, B.; Bazan, G. C.; Van Keuren, E.; *et al.* Endohedral Fullerenes for Organic Photovoltaic Devices. *Nat. Mater.* **2009**, *8*, 208–212.
4. Plant, S. R.; Ng, T. C.; Warner, J. H.; Dantelle, G.; Ardavan, A.; Briggs, G. A. D.; Porfyrakis, K. A Bimetallic Endohedral Fullerene: PrSc@C_{80}. *Chem. Commun.* **2009**, 4082–4084.
5. Suenaga, K.; Okazaki, T.; Hirahara, K.; Bandow, S.; Kato, H.; Taninaka, A.; Shinohara, H.; Iijima, S. High-Resolution Electron Microscopy of Individual Metallofullerene Molecules on the Dipole Orientations in Peapods. *Appl. Phys. A: Mater. Sci. Process.* **2003**, *76*, 445–447.
6. Chuvilin, A.; Khlobystov, A. N.; Obergfell, D.; Haluska, M.; Yang, S.; Roth, S.; Kaier, U. Observations of Chemical Reactions at the Atomic Scale: Dynamics of Metal-Mediated Fullerene Coalescence and Nanotube Rupture. *Angew. Chem., Int. Ed.* **2010**, *49*, 193–196.
7. Crewe, A. V.; Wall, J.; Langmore, J. Visibility of Single Atoms. *Science* **1970**, *168*, 1338–1340.
8. Nellist, P. D.; Pennycook, S. J. Direct Imaging of the Atomic Configuration of Ultra-Dispersed Catalysts. *Science* **1996**, *274*, 413–415.
9. Egerton, R. F. *Electron Energy-Loss Spectroscopy in the Electron Microscope*, 2nd ed.; Plenum Press: New York, 1996.
10. Crespi, V.; Chopra, N. G.; Cohen, M. L.; Zettl, A.; Louie, S. G. Anisotropic Electron-Beam Damage and the Collapse of Carbon Nanotubes. *Phys. Rev. B* **1996**, *54*, 5927–5931.
11. Varlot, K.; Martin, J. M.; Quet, C. EELS Analysis of PMMA at High Spatial Resolution. *Micron* **2001**, *32*, 371–378.
12. Smith, B. W.; Luzzi, D. E. Electron Irradiation Effects in Single Wall Carbon Nanotubes. *J. Appl. Phys.* **2001**, *90*, 3509–3515.
13. Egerton, R. F.; M Takeuchi, M. Radiation Damage to Fullerite (C_{60}) in the Transmission Electron Microscope. *Appl. Phys. Lett.* **1999**, *75*, 1884–1886.
14. Krivanek, O. L.; Chisholm, M. F.; Nicolosi, V.; Pennycook, T. J.; Corbin, G. J.; Dellby, N.; Murfitt, M. F.; Own, C. S.; Szilagyi, Z. S.; Oxley, M. P.; *et al.* Atom-by-Atom Structural and Chemical Analysis by Annular Dark Field Electron Microscopy. *Nature* **2010**, *464*, 571–574.
15. Meyer, J. C.; Kisielowski, C.; Erni, R.; Rossell, M. D.; Crommis, M. F.; Zettl, A. Direct Imaging of Lattice Atoms and Topological Defects in Graphene Membranes. *Nano Lett.* **2008**, *8*, 3582–3586.
16. K Suenaga, K.; Sato, Y.; Liu, Z.; Kataura, H.; Okazaki, T.; Kimoto, K.; Sawada, H.; Sasaki, T.; Omoto, K.; Tomita, T.; *et al.* Visualizing and Identifying Single Atoms Using Electron Energy-Loss Spectroscopy with Low Accelerating Voltage. *Nat. Chem.* **2009**, *1*, 415–418.
17. Warner, J. H.; Ito, Y.; Rümmeli, M. H.; Gemming, T.; Büchner, B.; Shinohara, H.; Briggs, G. A. D. One-Dimensional Confined Motion of Single Metal Atoms inside Double-Walled Carbon Nanotubes. *Phys. Rev. Lett.* **2009**, *102*, 195504-1–195504-4.
18. Dellby, N.; Krivanek, O. L.; Nellist, P. D.; Batson, P. E.; Lupini, A. R. Progress in Aberration-Corrected Scanning Transmission Electron Microscopy. *J. Electron Microsc.* **2001**, *50*, 177–185.
19. Cowley, J. M. Image Contrast in Transmission Scanning Electron Microscope. *Appl. Phys. Lett.* **1969**, *15*, 58–59.
20. Kato, H.; Taninaka, A.; Sugai, T.; Shinohara, H. Structure of Missing-Caged Metallofullerene: La_2@C_{72}. *J. Am. Chem. Soc.* **2003**, *125*, 7782–7783.
21. Stevenson, S.; Burbank, P.; Harich, K.; Sun, Z.; Dorn, H. C. La_2@C_{72}: Metal-Mediated Stabilization of a Carbon Cage. *J. Phys. Chem. A* **1998**, *102*, 2833–2837.
22. L Dunsch, L.; Bartl, A.; Georgi, P.; Kuran, P. New Metallofullerenes in the Size Gap of C_{70} to C_{82}: From La_2@C_{72} to Sc_3N@C_{80}. *Synth. Met.* **2001**, *121*, 1113–1114.
23. Yamanda, M.; Wakahara, T.; Tsuchiya, T.; Maeda, Y.; Akasaka, T.; Mizorogi, N.; Nagase, S. Spectroscopic and Theoretical Study of Endohedral Dimetallofullerene Having a Non-IPR Fullerene Cage: Ce_2@C_{72}. *J. Phys. Chem. A* **2008**, *112*, 7627–7631.
24. Ding, J.; Yang, S. Isolation and Characterization of Pr@C_{82} and Pr@C_{80}. *J. Am. Chem. Soc.* **1996**, *118*, 11254–11257.
25. Kucheyev, S. O.; Clapsaddle, B. J.; Wang, Y. M.; van Buuren, T.; Hamza, A. V. Electronic Structure of Nanoporous Ceria for X-ray Absorption Spectroscopy and Atomic Multiplet Calculations. *Phys. Rev. B* **2007**, *76*, 235420-1–235420-5.
26. P Trebbia, P.; Colliex, C. Study of the Excitation of 4d Electrons in Rare-Earth Metals by Inelastic Scattering of a High Energy Electron Beam. *Phys. Status Solidi B* **1973**, *58*, 523–532.
27. Ahn, C. C.; Krivanek, O. L. *EELS Atlas*; Gatan, Inc.: Warrendale, PA.
28. Khlobystov, A. N.; Britz, D. A.; Briggs, G. A. D. Molecules in Carbon Nanotubes. *Acc. Chem. Res.* **2005**, *38*, 901–909.